

# Investigation of grain refinement in Al/Al<sub>2</sub>O<sub>3</sub>/B<sub>4</sub>C nano-composite produced by ARB



Hossein Akbari beni<sup>a</sup>, Morteza Alizadeh<sup>a,\*</sup>, Mohammad Ghaffari<sup>b</sup>, Rasool Amini<sup>a</sup>

<sup>a</sup> Department of Materials Science and Engineering, Shiraz University of Technology, Modarres Blvd., 71555-313 Shiraz, Iran

<sup>b</sup> Department of Electrical and Electronics Engineering, UNAM-National Institute of Materials Science and Nanotechnology, Bilkent University, Ankara 06800, Turkey

## ARTICLE INFO

### Article history:

Received 26 February 2013

Received in revised form 10 September 2013

Accepted 25 October 2013

Available online 7 November 2013

### Keywords:

A. Metal–matrix composites (MMCs)

B. Microstructure

D. Electron microscopy

## ABSTRACT

In this study, Al/Al<sub>2</sub>O<sub>3</sub>/B<sub>4</sub>C nano-composites were fabricated via the accumulative roll bonding (ARB) process. The grain refinement of the Al/Al<sub>2</sub>O<sub>3</sub>/B<sub>4</sub>C nano-composite strips during the ARB process was studied. Microstructural characterizations of the fabricated composites after 2, 5, and 9 cycles were performed by transmission electron microscopy (TEM). The results showed that the composite sample, after 9 cycles, was filled with homogeneously distributed ultra fine grains with an average grain size of 230 nm. The findings also revealed that the increase in the dislocation density due to the presence of the nano-sized particles resulted in the grain refinement of the specimens. It was also found that the grain refinement is accelerated by the presence of the refinement particles.

© 2013 Elsevier Ltd. All rights reserved.

## 1. Introduction

Ultra-fine grained (UFG) materials with very small grains (smaller than 1 μm) and outstanding mechanical properties have been the focus of a considerable amount of research for potential use in structural materials in the industry [1,2]. UFG materials have found a wide range of usage in different fields such as automotive, aerospace and engineering applications [1,2]. This includes ultra-fine grained metal matrix composites (UFGMMCs) which can be used in important applications such as structural neutron absorbers, armor plate materials, and also as a substrate material for computer hard disks [3,4]. In particular, particle reinforced Al matrix composites have excited a good deal of interest due to its attractive properties such as being light weight, having a high elastic modulus and wear resistance, having a low thermal expansion coefficient, and the possibility of fabrication by many well-known methods [5]. The mechanical properties of these materials are highly dependent on following parameters: (a) the particle characteristics, (b) the particle distribution, and (c) the matrix mean grain size [6]. It has been reported that the mechanical properties of these materials can be improved by grain refinement [7]. Depending on the metal matrix, size and volume fraction of particles, and work conditions, different types of grain refinement can occur in the UFG materials [8–11].

To date, much research for obtaining a nano-scale ultra-fine microstructure has been done utilizing various severe plastic

deformation (SPD) processes, such as equal channel angular pressing (ECAP) [12], high pressure torsion (HPT) [13,14], accumulative roll-bonding (ARB) [15]. In the mentioned SPD processes, the ARB process has good potential to fabricate the material in the form of sheets. Recently, this process has been widely applied for production of UFG materials, such as Al, Al alloys [15,16], Mg [17], and some metal matrix composites (MMCs) [10,18]. It has been found that the formation mechanism of UFG by ARB is explained in terms of grain subdivision at a submicron scale [19–21]. In fact, grain refinement during the ARB process occurs by continuous fragmentation of the microstructure. The fragmentation results in the formation of low angle boundaries (LABs), which may eventually convert to high angle boundaries (HABs) [22]. In the ARB process, the formation of a large fraction of HABs at rolling stages can considerably refine the microstructure, whereby the mean grain size is reduced to a few hundred nanometers. The addition of nano-sized reinforcement ceramic particles to the matrix during the ARB process increases the fraction of HABs in the microstructure and accelerates grain refinement [6]. Furthermore, the microstructure is affected by the particle volume fraction. Kang and Chan [7] indicated that by increasing the reinforcement nano-particles from 0 to 4 vol.%, the average grain size of the matrix decreases and its strength is increases. However, as the content of reinforcement exceeded 4 vol.%, the average grain size remained unchanged and the strengthening effect leveled off because of the clustering of the reinforcement [7]. In the present work, we attempt to explain grain refinement mechanisms of alumina and boron carbide nano-particles reinforced aluminum matrix composite (Al/Al<sub>2</sub>O<sub>3</sub>/B<sub>4</sub>C).

\* Corresponding author. Tel.: +98 711 7278491; fax: +98 711 7354520.

E-mail address: [Alizadeh@sutech.ac.ir](mailto:Alizadeh@sutech.ac.ir) (M. Alizadeh).

The microstructural evolution during the ARB process was investigated by TEM.

## 2. Experimental

As-received commercial purity aluminum sheets (specifications are given in Table 1),  $\text{Al}_2\text{O}_3$  and  $\text{B}_4\text{C}$  particles (with an average size of 50 nm) were used as raw materials. Strips of 1050-aluminum were cut into  $200 \text{ mm} \times 40 \text{ mm} \times 0.5 \text{ mm}$  pieces parallel to the rolling direction and were annealed at 623 K in an ambient atmosphere. The strips were degreased in acetone and scratch brushed with a 90 mm diameter stainless steel circumferential brush with a 0.35 mm wire diameter and surface speed of  $14 \text{ m s}^{-1}$ . To fabricate the composites by the ARB process, four strips were stacked over each other to achieve a 2 mm thickness, while about 1.3 wt.%  $\text{Al}_2\text{O}_3$  and  $\text{B}_4\text{C}$  powders were dispersed between each of the two layers (Fig. 1(a)). The stacked strips were fastened at both ends by steel wire to prepare it for the rolling process. The strips were roll-bonded with draft percentage of 50% reduction (von Mises equivalent strain of 0.8) in one cycle at room temperature. In this cycle, which was named first cycle, the number of  $\text{Al}_2\text{O}_3$ – $\text{B}_4\text{C}$  layers was three and the number of aluminum layers was four. In the next step, the well roll-bonded strip was cut into two strips by a shearing machine and degreased in acetone, scratch brushed and after stacking over each other, without  $\text{Al}_2\text{O}_3$ – $\text{B}_4\text{C}$  particles between them, were roll-bonded with a draft percentage of 50% reduction once again. The last step of the process was repeated up to nine cycles without annealing between each cycle (Fig. 1(b)). After nine accumulative roll-bonding cycles in total, the Al matrix composite, including the well dispersed  $\text{Al}_2\text{O}_3$ – $\text{B}_4\text{C}$  reinforcements, was produced. The ARB experiments were carried out, without lubricant, using a laboratory rolling mill with a loading capacity of 20 tons. The roll diameter was 230 mm, and the rolling speed ( $\omega$ ) was 15 rpm ( $133.44 \text{ mm s}^{-1}$ ). The microstructural observations were performed using transmission electron microscopy (Philips-FEG). The TEM samples after ARB process were prepared by using electrolytical thinning in an electrolyte consisting of 1/3  $\text{HNO}_3$  2/3  $\text{CH}_3\text{OH}$  at subzero temperatures. Thin foils parallel to the rolling plane (rolling direction–transverse direction or RD–TD plane) were prepared by the ion milling technique.

## 3. Result and discussion

The microstructural changes of the Al/ $\text{Al}_2\text{O}_3$ /B<sub>4</sub>C nano-composite during the ARB process was investigated by TEM. Fig. 2 demonstrates the TEM microstructure and the corresponding selected area diffraction patterns (SAD) of the aluminum matrix observed in RD–TD plane of the Al/ $\text{Al}_2\text{O}_3$ /B<sub>4</sub>C nano-composite after the 2nd, 5th, and 9th cycles. It is clear that the ARB process leads to a significant refinement of the microstructure after nine ARB cycles. In the SAD pattern of the deformed sample after 2 cycles, distinct spots indicate that the area has low misorientation. The TEM analysis of this sample (Fig. 2a) shows bright and dark contrast changes which suggest the formation of low angle boundaries. Therefore, the grain structure at this stage mainly consists of subgrains with a dislocation cell structure. The presence of the  $\text{B}_4\text{C}$  and  $\text{Al}_2\text{O}_3$  particles in the Al matrix is responsible for an increase of the dislocation density and accelerated formation of subgrains and the dislocation cell structure. It has been reported

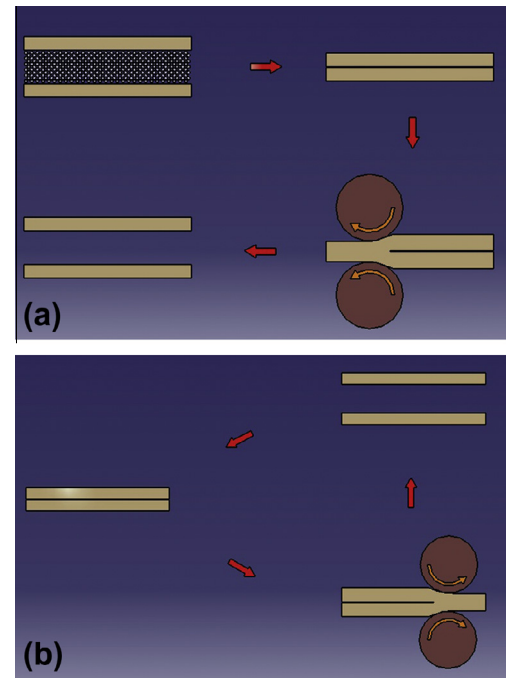
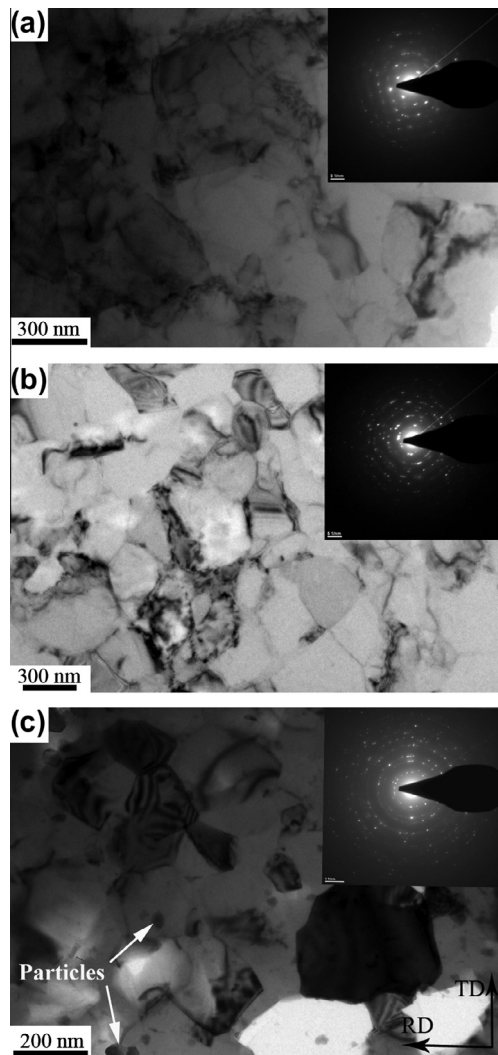


Fig. 1. Schematic illustration of the production process of the Al/ $\text{Al}_2\text{O}_3$ – $\text{B}_4\text{C}$  nano-composite sheets through the ARB process: the first step (a) and the second step (b).

that these dislocations are generated at particle–matrix interfaces to accommodate strain incompatibility [23]. In addition, they are generated because of the difference in the coefficients of thermal expansion between the matrix and reinforcing particles [17]. Eventually, the microstructure after a second cycle shows a mixture of deformed-non deformed grains with some regions of dislocation tangles, dislocation cells, and dense dislocation walls. The average size of these grains that were measured by the intercept method is about 700 nm. As it can be seen from Fig. 2b, after the 5th cycle, the microstructure became more uniform and some grains with an average grain size of 500 nm are formed. In this cycle the dislocation density is increased, whereas it decreases within the cells due to movement and accumulation of dislocations in the boundaries and consequently, cell size became finer in comparison to the 2nd cycle. The grain structure of the specimen at this stage consisted of subgrains divided by dislocation walls. In fact, in this case, plenty of geometrically-necessary (g-n) dislocations are introduced around the  $\text{Al}_2\text{O}_3$ /B<sub>4</sub>C particles (to justify their interfaces with the metallic phase) and the fraction of low angle grain boundaries increases [18]. By comparing Fig. 2a and b it can be seen that the SAD pattern in Fig. 2b is more diffuse than the former SAD pattern and gradually evolves into a ring pattern consisting of extra spots which is an indication of large misorientation. With increasing the strain to 9 cycles, the specimen was filled with the homogeneous distribution of ultra-fine grains surrounded by high-angle boundaries with average size of 230 nm (see Fig. 2c). It is obvious that with the progression of the ARB process, the fraction of the ultra-fine grained regions increases. The ring-like shape of the selected area diffraction pattern shown in Fig. 2c confirms the presence of a high portion of high angle boundaries in this cycle. In other words, the SAD pattern indicates that large local

Table 1  
Chemical composition of the 1050 Al alloy.

Element	Al	Si	Fe	Cu	Mg	Zr	Ti	Cr	Ni
wt.%	99.344	0.1	0.43	0.09	0.02	0.0008	0.005	0.0016	0.0014



**Fig. 2.** TEM microstructure and associated selected area diffraction (SAD) pattern of the Al/Al<sub>2</sub>O<sub>3</sub>-B<sub>4</sub>C nano-composite after 2, 5, and 9 cycles.

misorientation exists between the ultra- fine grains. According to TEM results, it is evident the subgrain and dislocation cell structures with low angle grain boundaries are formed at first and the misorientation at low angle boundaries of the subgrain and dislocation cell structures is increased by progression of the ARB process. Finally, after of nine cycles, an UFG is achieved in the specimen. Various major factors which affect the grain refining of Al/Al<sub>2</sub>O<sub>3</sub>/B<sub>4</sub>C nano-composite produced by the ARB process includes wire-brushing, large shear strain, nano-particles, and temperature rise. These factors will be discussed in the subsequent sections.

### 3.1. Effect of wire-brushing on the grain refinement

It has been reported that to create a satisfactory metallurgical bond in the roll welding process, it is essential to remove contamination layers (such as oxides, grease, and dust particles) between the surfaces of the two metals to be joined [24]. The wire brushing process can be used for removing oxide layers from Al surface. In addition, the wire brushing process is used for creation of a hard surface layer on the strips and has a significant role in grain refinement of strip surfaces in the ARB process [25]. Recently, the wire brushing process has been utilized for surface modification of alloys. For instance, Kitahara et al. [25] has used the wire-brushing

process for the purpose of surface grain refinement. They have reported that the grain refinement may result from the plastic flow during wire-brushing, such as friction stir welding. In the ARB process the wire brush introduces a severe local shear strain on the strip's surface and the dislocation density is locally increased and results in grain refinement. It should be noted that the grain refinement fraction in the surface of the Al/Al<sub>2</sub>O<sub>3</sub>/B<sub>4</sub>C nano-composite is affected by the wire-brushing load.

### 3.2. Effect of large shear strain on the grain refinement

During the ARB process, due to the frictional effects between rolls surfaces and the surface of the sample under non-lubricated conditions, an additional shear strain (redundant shear strain) is introduced near the sample's surface whose direction is parallel to the rolling direction [20]. Therefore, the deformation at the surface is a combination of the theoretical and frictional shear. This additional shear near the surface has an important effect on the microstructure [20]. Additional shear may increase the strain near the sample surface above the nominal strain imposed during the ARB process. Therefore, it can be expected that in the vicinity of the surface, the microstructural evolution occurs more rapidly than closer to the center of the sample. In the ARB process, owing to repetition of cutting, stacking and roll-bonding, a complicated frictional shear distribution is expected through the sheet thickness and results in microstructural heterogeneity throughout the thickness [20]. The important role of the frictional shear to the microstructural evolution was also reported for some others severe plastic deformation methods such as the ECAP process [12]. It has been reported that because of frictional shear, the rate of microstructure evolution in Al during the ARB process is higher than that in conventional cold rolling even after the same rolling reduction [12].

### 3.3. Effect of nano-particle on the grain refinement

Fig. 3 illustrates the TEM microstructure of the Al/Al<sub>2</sub>O<sub>3</sub>/B<sub>4</sub>C nano-composite and monolithic Al after 5 ARB cycles. Comparison of these images reveals the important role of the hard particles on grain refining of the matrix during the ARB process. In this case the grain refinement process is augmented when Al<sub>2</sub>O<sub>3</sub> and B<sub>4</sub>C nano-particles are added to the Al matrix. The grain refinement during the ARB process of the Al/Al<sub>2</sub>O<sub>3</sub>/B<sub>4</sub>C nano-composite is attributed to hard ceramic particles that can be explicated on the basis of enhanced dislocation density whereas they can lead to an increased rate in the generation of HAGB areas with strain. As such, a submicron grain structure can be obtained at a considerably lower strain than that of the single-phase alloy [22]. The reasons for the increase of dislocation density can be listed as follows:

1. During the ARB process, the dislocations are probably generated at the Al<sub>2</sub>O<sub>3</sub> and B<sub>4</sub>C nano-particles/matrix interface to accommodate strain incompatibility between the two phases. Fig. 4 shows the presence of the generated dislocations in the particles/matrix interface. In fact, the presence of these hard particles results in increased local strain of the matrix in the proximity of the particles which enhances the work hardening of the matrix, in comparison with the unreinforced Al [10,26].
2. Because of the difference between the thermal expansion coefficients (CTE) of the reinforcements and the matrix ( $26.49 \times 10^{-6}/\text{K}$  for Al,  $5 \times 10^{-6}/\text{K}$  for Al<sub>2</sub>O<sub>3</sub> and  $8.1 \times 10^{-6}/\text{K}$  for B<sub>4</sub>C) on cooling from the processing temperature, thermal stresses around the nano-particles that large enough to cause plastic deformation are generated in the matrix, especially in the interface region [27]. These stresses decrease quickly with



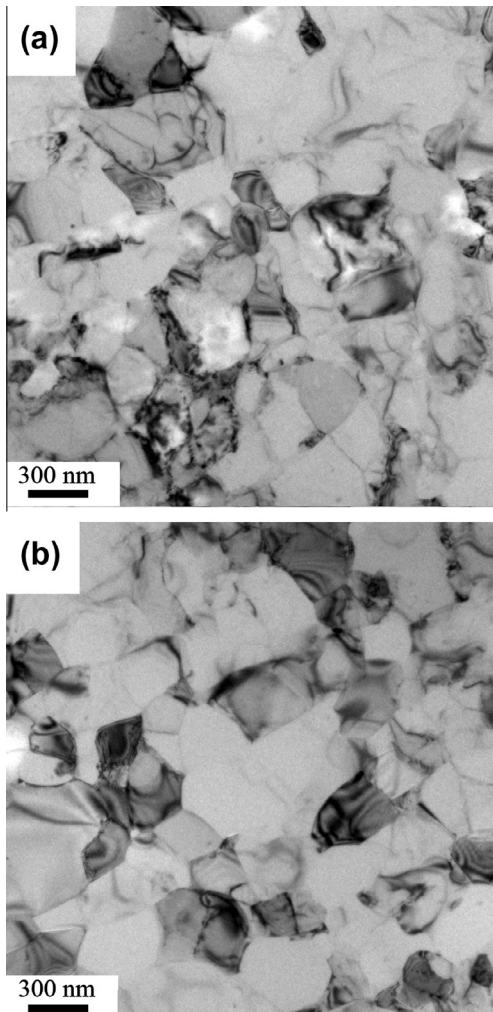


**Fig. 3.** TEM microstructure of the Al/Al<sub>2</sub>O<sub>3</sub>-B<sub>4</sub>C nano-composite (a) and the monolithic Al (b) after 5 cycles.

increasing distance from the boundary, which can generate small defects such as dislocations in the close vicinity of nano-sized particles.

3. During deformation, fine reinforcement particles are known to increase the rate of dislocation generation by encouraging the formation of Orowan loops [28]. This will increase the work hardening rate and dislocation density [28], which is more dependent on heterogeneous features. In fact, since the particles are strong enough to resist the passage of dislocation, the Orowan loops may be formed [28]. During the ARB process, due to continued deformation, more loops will form and the resulting stress will be local plastic flow or plastic relaxation in the matrix to relieve these stresses. At large strains, more complex dislocation structures are deformed and these are often associated with local lattice rotations close to the particles, and such regions are commonly formed plastic deformation zones. Finally, plastic relaxation occurs by the formation of rotated deformation zones (Fig. 5).

Another mechanism in the grain refining in this study is pinning of the grain boundaries by alumina and boron carbide particles and particles of oxide film [10]. After several cycles of the ARB process, a large number of interfaces are introduced. The alumina and boron carbide particles and the oxide films formed on the surfaces act as obstacles for grain growth (Fig. 6). Both the inserted particles

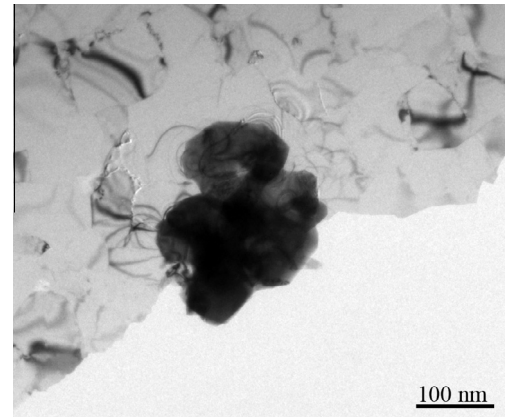


**Fig. 4.** TEM micrograph showing generation of the dislocation in near reinforcement.

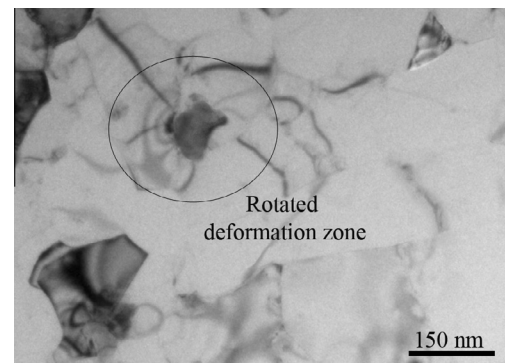


**Fig. 5.** TEM micrograph showing rotated deformation zone.

and oxides can be considered obstacles to the dislocation motion, and therefore create dislocation accumulations [10]. The dislocation rearrangements lead to the formation of subgrain boundaries. High dislocation density is due to the intense stress and higher rate of diffusion in the area so that the subgrain boundaries further evolve into grain boundaries with large angles of misorientation.

### 3.4. Effect of temperature rise on the grain refinement

Lee et al. [9] explained that the continuous changes in misorientation are turned into the planar boundaries by rearrangement of the geometrically necessary (g-n) dislocations by short-range diffusion. Short-range diffusion is possible even at ambient temperature due to the temperature rise by plastic work. The temperature rise of deforming metal,  $\Delta T$ , by plastic work has been estimated by Lee et al. [9]:

$$\Delta T = \frac{\eta \varepsilon \sigma}{\rho C} \quad (1)$$

where  $\eta$  is the efficiency of mechanical work,  $\sigma$  is mean flow stress,  $\varepsilon$  is equivalent strain,  $\rho$  is density of metal and  $C$  is the specific heat of deforming material. It has been reported [18] that the calculated temperature rise was 50 K from the first to the third ARB cycle and 90 K at the fourth cycle, and it was about 110 K after the sixth cycle. The actual temperature rise is definitely higher than these calculated values firstly in this case, alumina and boron carbide have a very low thermal conductivity (30 and 35 W/m K respectively) while aluminum has a high thermal conductivity (250 W/m K) [10]. Secondly, the contribution of the frictional heat between the rolls and work-piece on the temperature increase is neglected.

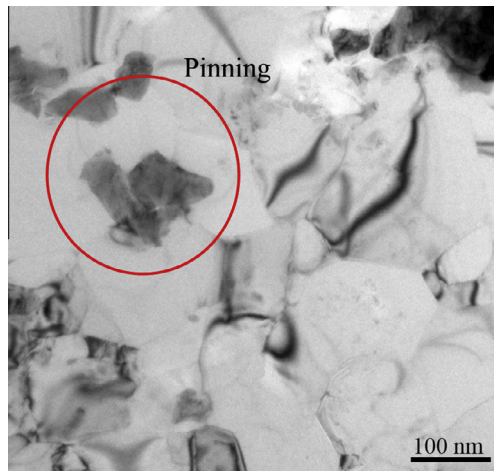


Fig. 6. TEM micrograph showing effect pinning of the particles.

Therefore, as mentioned above, short-range diffusion can occur even at room temperature which promotes the formation of an ultra-fine grained structure.

#### 4. Conclusion

In this study, Al/Al<sub>2</sub>O<sub>3</sub>/B<sub>4</sub>C nano-composites and monolithic Al were fabricated in the form of sheets via the ARB process, and the effect of the Al<sub>2</sub>O<sub>3</sub>/B<sub>4</sub>C nano-particles on the microstructure evolution during the ARB process was investigated. The conclusions drawn from the results can be summarized as follows:

1. The ultra fine grained Al/Al<sub>2</sub>O<sub>3</sub>/B<sub>4</sub>C composites with average grain size of 230 nm were fabricated by the ARB process after nine cycles.
2. Microstructural characterization shows that finer matrix grain size can be obtained with the presence of nano-Al<sub>2</sub>O<sub>3</sub>/B<sub>4</sub>C particles in comparison with monolithic Al.
3. The presence of the nano-Al<sub>2</sub>O<sub>3</sub>/B<sub>4</sub>C particles in the aluminum matrix lead to significant increase in dislocation density.
4. The nano-Al<sub>2</sub>O<sub>3</sub>/B<sub>4</sub>C particles accelerate grain refinement during the ARB process.
5. Orowan mechanism is found to play a significant role in grain refinement of MMNCs.

#### Acknowledgment

The authors gratefully acknowledge the financial support received from Iran National Science Foundation (INSF).

#### References

- [1] Manoharan M, Gupta M. Effect of silicon carbide volume fraction on the work hardening behavior of thermo mechanically processed aluminium-based metal–matrix composites. *Composites Part B* 1999;30:107–12.
- [2] Zhou Z, Wang Z, Yi Y, Jiang S, Wang G, Chen J. Properties and micro-structure of ZrO<sub>2</sub>–Al<sub>2</sub>O<sub>3</sub> composites with three-layer structure. *Composites Part B-Eng* 2011;42:1271–5.
- [3] Alizadeh M. Comparison of nanostructured Al/B<sub>4</sub>C composite produced by ARB and Al/B<sub>4</sub>C composite produced by RRB process. *J Alloys Compd* 2010;528:578–82.
- [4] Alizadeh M, Paydar MH, Sharifan F. Structural evaluation and mechanical properties of nanostructured Al/B<sub>4</sub>C composite fabricated by ARB process. *Composites Part B-Eng* 2013;44(1):339–43.
- [5] Kaczmar JW, Pietrzak K, Wlosinski W. The production and application of metal matrix composite materials. *J Mater Process Technol* 2000;106:58–67.
- [6] Schmidt CW, Knieke C, Maier V, Höppel HW, Peukert W, Göken M. Accelerated grain refinement during accumulative roll banding by nanocomposite reinforcement. *Scr Mater* 2011;64:245–8.
- [7] Kang YC, Chan SL. Tensile properties of nanometric Al<sub>2</sub>O<sub>3</sub> particulate-reinforced aluminum matrix composites. *Mater Chem Phys* 2004;85:438–43.
- [8] Shaarabaf M, Toroghinejad MR. Nano-grained copper strip produced by accumulative roll bonding process. *Mater Sci Eng A* 2008;473:28–33.
- [9] Lee SH, Saito Y, Sakai T, Utsunomiya H. Microstructures and mechanical properties of 6061 aluminum alloy processed by accumulative roll-bonding. *Mater Sci Eng A* 2002;325:228–35.
- [10] Jamaati R, Toroghinejad MR, Dutkiewicz J, Szpunar JA. Texture evolution of nanostructured aluminum/copper composite produced by the accumulative roll bonding and folding process. *Mater Des* 2012;35:37–42.
- [11] Alizadeh M, Paydar MH. High-strength nanostructured Al/B<sub>4</sub>C composite processed by cross-roll accumulative roll bonding. *Mater Sci Eng A* 2012;538:14–9.
- [12] Reihanian M, Ebrahimi R, Tsuji N, Moshksar MM. Analysis of the mechanical properties and deformation behavior of nanostructured commercially pure Al processed by equal channel angular pressing (ECAP). *Mater Sci Eng A* 2008;473:189–94.
- [13] Azushima A, Kopp R, Korhonen A, Yang DY, Micari F, Lahoti GD, et al. Severe plastic deformation (SPD) processes for metals. *CIRP Ann-Manuf Technol* 2008;57:716–35.
- [14] Valiev RZ. Structure and mechanical properties of ultrafine grained metals. *Mater Sci Eng A* 1997;234–236:59–66.
- [15] Saito Y, Utsunomiya H, Tsuji N, Sakai T. Novel ultra-high straining process for bulk materials –development of the accumulative roll-bonding (ARB) process. *Acta Mater* 1999;47:579–83.
- [16] Pirgazi H, Akbarzadeh A, Petrov R, Kestens L. Microstructure evolution and mechanical properties of AA1100 aluminum sheet processed by accumulative roll bonding. *Mater Sci Eng A* 2008;497:132–8.
- [17] Hassan SF, Gupta M. Development of high strength magnesium copper based hybrid composites with enhanced tensile properties. *Compos Struct* 2006;72:19–26.
- [18] Alizadeh M, Paydar MH. Fabrication of nanostructure Al/SiC<sub>p</sub> composite by accumulative roll-bonding (ARB) process. *J Alloys Compd* 2010;492:231–5.
- [19] Utsunomiya H, Tanda K, Saito Y, Sakai T, Tsuji N. Effects of lubrication on accumulative roll-bonding (ARB) of aluminum. *J Jpn Soc Technol Plast* 1999;40:1187–91.
- [20] Lee SH, Saito Y, Tsuji N, Utsunomiya H, Sakai T. Role of shear strain in ultra grain refinement by accumulative roll-bonding (ARB) process. *Scr Mater* 2002;46:281–5.
- [21] Liu Q, Hansen N. Macroscopic and microscopic subdivision of a cold-rolled aluminium single crystal of cubic orientation. *Proc R Soc Lond A* 1998;454:2555–91.
- [22] Quadir MZ, Ferry M, Munroe PR. The initial stages of formation of low angle boundaries within lamellar bands during accumulative roll bonding of aluminum. *Scr Mater* 2011;64:1106–9.
- [23] Tsuji N, Toyoda T, Minamino Y, Koizumi Y, Yamane T, Komatsu M, et al. Microstructural change of ultrafine grained aluminum during high-speed plastic deformation. *Mater Sci Eng A* 2003;350:108–16.
- [24] Alizadeh M. Effects of temperature and B<sub>4</sub>C content on the bonding properties of roll-bonded aluminum strips. *J Mater Sci* 2012;47:4689–95.
- [25] Kitahara H, Yada T, Tsushidab M, Andoa S. Microstructure and evaluation of wire-brushed Mg sheets. *Pro Eng* 2011;10:2737–42.
- [26] Alizadeh M, Akbari beni H, Ghaffari M, Amini R. Properties of high specific strength Al–4 wt.% Al<sub>2</sub>O<sub>3</sub>/B<sub>4</sub>C nano-composite produced by accumulative roll bonding process. *Mater Des* 2013;50:427–32.
- [27] Zhang Z, Chen DL. Consideration of Orowan strengthening effect in particulate-reinforced metal matrix nanocomposites: a model for predicting their yield strength. *Scr Mater* 2006;54:1321–6.
- [28] Apps PJ, Berta M, Prangnell PB. The effect of dispersoids on the grain refinement mechanism during deformation of aluminum alloys to ultra-high strains. *Acta Mater* 2005;53:499–599.